This is the preprint of the contribution published as:

Rosa, L.F.M., **Röhring, K.**, **Harnisch, F.** (2024):
Electrolysis of medium chain carboxylic acids to aviation fuel at technical scale
Fuel **356** , art. 129590

The publisher's version is available at:

https://doi.org/10.1016/j.fuel.2023.129590

Electrolysis of medium chain carboxylic acids to aviation fuel at technical scale

Luis F. M. Rosa[1,&,$], Katharina Röhring[1,$] & Falk Harnisch[1,*]

[1] Department of Environmental Microbiology, Helmholtz-Centre for Environmental Research – UFZ, Permoserstraße 15, 04318 Leipzig, Germany

[$] current affiliation: King Abdullah University of Science and Technology (KAUST), Thuwal, Kingdom of Saudi Arabia

*corresponding author (falk.harnisch@ufz.de)

[$]both authors contributed equally

Abstract

For mobility, especially in aviation, cargo weight and volume of the energy-vector are substantially more limited than in any other form of transportation. Therefore, energy vectors with high mass and volume specific energy density are needed, for which carbon-based liquid fuels are unmatched. Concurrently, there is an imperative of deriving these fuels from non-fossil sources. Here, we show the scale-up of the production of aviation drop-in fuel-like mixtures (mainly *n*-decane) that are obtained by Kolbe electrolysis of medium chain carboxylic acids (*n*-hexanoic acid), which can be derived from biomass. We increased the scale to 1 L volume and 100 cm^2 electrode surface area within a single stack electrolysis cell allowing straightforward numbering-up. The obtained electrolysis performance is unprecedented at technical scale with a maximum *n*-decane production rate of 0.73 g L^{-1} h^{-1} cm^{-2}, a selectivity for *n*-decane between 76.3 % and 97.8 % and Coulombic efficiencies up to 68 %.

Key words: biobased drop-in fuel, electrolysis, electrofuels, electrochemical engineering, electrobiorefinieries

1. Introduction:

Transportation of goods and mobility of people are the main consumers of fossil carbon like oil or gas and among the prime emitters of greenhouse gases, especially CO_2. The transport sector is accountable for 16.2% of total CO_2 emissions, where road transport including cars, lorries, motorcycles and buses contributes with a share of 11.9%, and aviation - emissions from domestic and international passenger travel and freight shipping - contribute with 1.9%, followed by boat shipping which contributes with a 1.7% share [1]. Thus, humankind is seeking globally for renewable sources of energy for mobility and transportation at land, air and sea. Using electric energy as energy vector and its storage in batteries is the most popular approach for (individual) mobility at land, with electric cars increasing the market share of new car sales above 25% in Europe, US and China. Further, current EU legislation aiming to phasing out internal combustion engines in cars and small commercial delivery vehicles as soon as 2035 [2, 3]. Yet, using electric batteries for heavy transportation of goods is questionable. With battery energy requirements per truck reaching as high as 1 MWh (and as consequence, circa 4 Tons of battery per truck), the fast-charging power needs for a long hauling transport fleet would require circa 10% of the EU´s total electric power generation capacity [4]. As world-wide implementation of battery powered mobility will suffer from the availability and mining of scarce resources like Co, Mn, Ni, Li, we cannot foresee a full battery-based mobility infrastructure [5]. Awareness that batteries will not be the unique answer has recently led to a world-wide upswing for promoting hydrogen (H_2) as universal energy vector. H_2 possess undebatable advantages, most importantly of only emitting H_2O when being “burned” in an internal combustion engine or in fuel cells [6]. Yet, generating H_2 at large scale, for instance using electrolysis or photochemistry and photobiology, is far from being state of the art [7]. Additionally, it does also require precious resources like noble-metals for electrolysers or land for (biological) solar panels. The logistic of H_2 are also complex, as it is the smallest molecule in existence (as well as the lightest gas), requiring very high-tech (and costly) materials for its containers and extreme temperatures/pressures for its liquefaction and storage.

Further to the challenges and limitations that come with the technologies for their generation and storage of electric energy, batteries, hydrogen as well as other non-carbon based energy sources and vectors share one common limitation, their low mass related energy density. The mass related as well as volume related energy density of carbon based liquid fuels is unmatched [8]. The energy vector that is the “fuel” represents carry-on luggage and thus its weight limits the vehicle’s reach and the volume determines volumetric ratio

of “fuel-tank-volume” and “effective volume” that can be used for transportation. This creates a need for energy vectors with high mass and volume specific energy density. This is especially the case for aviation fuels [9, 10]. This clear rationale for the high relevance of carbon-based aviation fuels creates the need for deriving these from non-fossil sources. For instance, and by descending order of technology readiness level (TRL), the following types of fuels incl. drop-in fuels and additives are approved for usage in international aviation: synthetic paraffinic kerosene, hydroprocessed esters and fatty acids, alcohol-to-jet synthetic paraffinic kerosene, hydroprocessed fermented sugar synthesized iso-paraffins, Fischer-Tropsch synthetic paraffinic kerosene, pyrolysis oils and others [9, 11, 12].

Recently, we have shown that complex waste biomass can be converted to fuel-like mixtures using a combined microbial and electrochemical conversion process. This forms the foundation of the electrobiorefinery, concept displayed in Fig. 1. Providing proof-of-principle at 50 mL laboratory scale [13] Urban *et al.* showed successfully the conversion of corn beer to a hydrocarbon mixture used as potential diesel additive at 0.48 g_{COD} g_{COD}^{-1} [hydrocarbon/corn beer, displayed in equivalents of chemical oxygen demand (COD)] with a two-stage process. Here, mainly the composition of the intermediate medium chain carboxylic acids (MCCA) that are produced by the biological stage influenced the outcome of the electrochemical conversion. Furthermore, Urban *et al.* proposed that the full potential of the presented process can only be exploited if the individual process steps are subjected to engineering and scale-up.

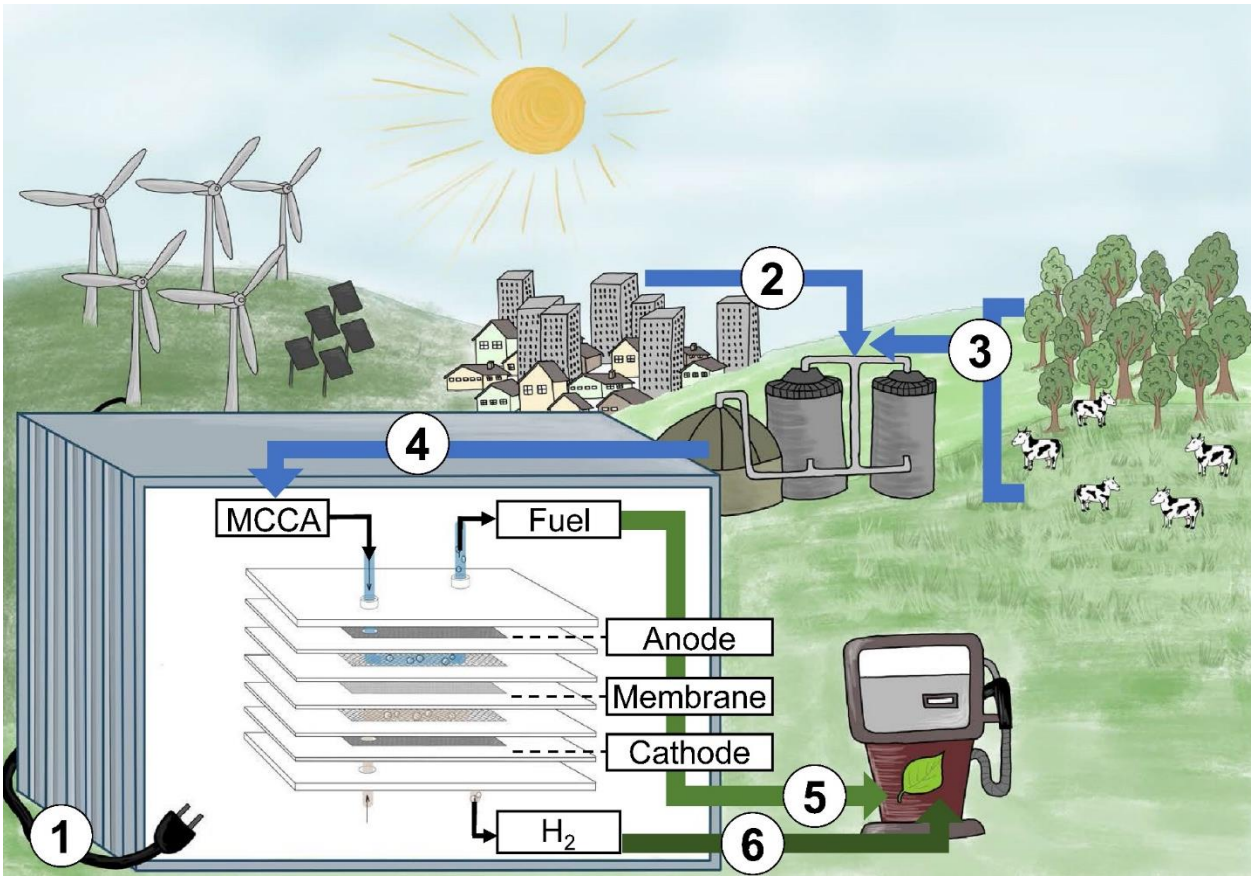


Figure 1: Scheme of an electrobiorefinery for conversion of waste biomass into bio-based fuel. Blue arrows indicate the process line of the waste biomass and the green arrows indicate the final electrochemical products that can be used as fuel. 1: renewable energy from e.g. solar or wind power used to power the electrochemical conversion, 2: urban waste biomass e.g. food waste, 3: agricultural and forestry waste e.g. peels, leaves or acid whey, 4: intermediate product (*medium chain carboxylic acids* - MCCA) from bioconversion (fermentation) as substrate for the electrochemical conversion, 5: final product of the electrochemical conversion (alkane mixture with fuel properties) used as bio-based fuel 6: H_2 produced at the cathode used for H_2 mobility.

For this two-stage process the biological conversion of biomass to MCCA is deeply researched and already developed towards technological scale. A variety of complex substrates such as corn beer [13], acid whey [14, 15] or other organic waste streams [16-18] can be converted to MCCA by anaerobic open-culture fermentation. Thereby, important process parameters for efficient MCCA production are the inhibition of competitive carbon-consuming pathways, prevention of substrate and product inhibition, pH and hydraulic

retention time (HRT) [16, 19-21]. Production rates of 9 g L^{-1} d^{-1} [18, 22] up to 52 g L^{-1} d^{-1} [20, 23] (maximum rates in n-C6 equivalents when assuming caproic acid as the only MCCA that is consuming 8 moles of O_2 per mole of acid for complete combustion) can be achieved for different MCCA, depending on the process management. This well-known biotechnological process is already performed at semi-pilot scale [24]. In contrast, there are mainly fundamental studies on the electrolysis which point to the importance of electrode material, reactant concentration and current density. The most recent studies of Kolbe electrolysis performed in a scale and conditions related to this study (36 cm^2 anode surface area, 1 L holding vessel), dates back more than 3 decades [25, 26]. Using a custom made, non-separated (no membrane) electrochemical cell and a platinum electrode little to no focus was put on the energetic optimization of the electrochemical reactions, but more on extended reaction yields form different MCCA mixtures. Thus, only a yield or degree of conversion was reported without commenting on CE or the energetic efficiency, yet this is almost of no value for any process characterization. Only in the recent years, since electrochemical synthesis has gained more interest in the context of a circular bioeconomy, the influence of various process parameters and architecture of electrochemical reactors has regained attention, also for improving energetic and process efficiency. These include, for instance, channel length[27], reactor design[28] and HRT[29] of electrochemical flow cells as well as the substrate composition[30], for the technical integration of the Kolbe electrolysis into existing biorefinery concepts. The Kolbe electrolysis enables the electrochemical upgrading of MCCA to a mixture of hydrocarbons, primarily alkanes, as shown in Fig. 2 using the example of *n*-hexanoic acid (C_6) that was also used in this study. This hydrocarbon mixture has fuel properties as previously shown in laboratory scale experiments by Urban *et al.* [13]. However, for a smooth integration of the Kolbe electrolysis into existing well-studied biological process lines its scaling-up is required. Here we demonstrate process feasibility in a commercially available single stack electrolysis cell, making future application of the Kolbe electrolysis possible as no further transfer from a tailor-made electrochemical device cell to a commercially available one that can be numbered up is necessary. Additionally, an economically viable anode material on the example of C_6 that is most extensively studied at laboratory scale was used [31, 32]. We provide complete data sets on the energetic efficiencies, yields and production rates for process characterization.

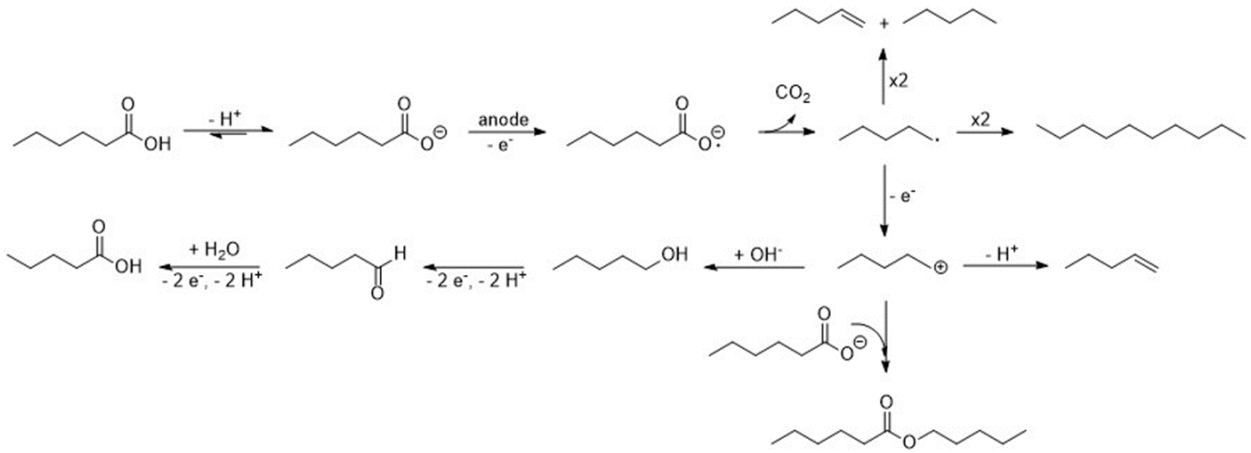


Figure 2: Reaction scheme showing the different possible reaction pathways of electrochemical decarboxylation of C_6 via Kolbe electrolysis [31].

2. Experimental

2.1. General Remarks

All chemicals were of at least analytical grade and are listed in the Supplementary material (SI section 2.1). All solutions were prepared with de-ionized water (Milli-Q IQ 7000, Merck KgaA, Darmstadt, Germany). A list of all used symbols and abbreviations can also be found in the SI (Tab. S1).

2.2. Single stack electrolysis cell

A single stack electrolysis cell, i.e. a two-chamber electrochemical flow cell (Electro MP Cell, ElectroCell Europe A/S, Tarm, Denmark, see Fig. S1), was used for scaling and process engineering of the Kolbe electrolysis on the example of converting *n*-hexanoic acid (C_6, see Fig. 2). The measured volume of anode as well as cathode chamber was 100 mL each, created by an 8 mm polypropylene spacer, equipped with a turbulence promoter mesh. Both electrodes were platinized titanium (Electro MP Cell, ElectroCell Europe A/S, Tarm, Denmark) and the liquid contact surface area of each electrode was 100 cm^2.

The implemented electrode surface area to volume ratio (100 cm^2 for 1 L solution) and high recirculation flow rate of 1 L min^{-1} with a recirculation time of 1 min for the total anode volume resembles batch conditions. This means that concentrations of substrates and products can be considered homogeneous in the

aqueous phase, whereas the organic phase (fuel) quickly phase-separates and accumulates inside the holding vessel (see Fig. S2). Thus, reactant and product concentrations inside the single stack electrolysis cell decreased. Even with vigorous stirring of the liquid in the holding vessel (500 rpm with a 2 L bioreactor Rushton turbine, not shown), complete homogeneity of aqueous and organic phase could not be achieved, thus not allowing for time point sampling. Thus, all electrolysis were run to specific endpoints without intermediate sampling.

All electrolysis were carried out galvanostatically using a DC power source (Model # PS9080-170, EA Elektro-Automatik GmbH & Co. KG, Viersen, Germany) with a two-electrode setup. The cell potential between WE and CE (E_{cell}) was measured using the DC power source. All electrolysis were started at room temperature. After each electrolysis both cell chambers were cleaned with warm (60 °C) tap water, followed by extensive rinsing with distilled water. Between electrolysis the reactor was flushed with distilled water at a low flow rate (100 mL min^{-1}).

2.3. Kolbe electrolysis

For Kolbe electrolysis 2 L of 0.5202 ± 0.0014 M *n*-hexanoic acid solution with 35 g L^{-1} Na_2SO_4 were prepared as anolyte. The pH of the anolyte was between 7.2 and 7.6 and the conductivity was 45 ± 3 mS cm^{-1}. The solution was then split in two times 1 L and used for independent electrolysis. The catholyte was MilliQ water, NaOH pellets and 35 g L^{-1} Na_2SO_4 to reach a similar pH and conductivity as the anolyte. 4 L of catholyte were reutilized for a maximum of three consecutive electrolysis. The electrolysis were carried out at different rates of conversion, i.e. current densities (150, 300, 450 mA cm^{-2}), and ran for different lengths of time until different degrees of conversion, i.e. Faraday equivalents (FE), were reached (0.25, 0.5, 1.0, 1.5). FE reflect the amount of charge required to convert a defined portion of the substrate assuming 100 % Coulombic efficiency as well as 100% selectivity of the corresponding reaction. For example, in the case of 0.5 FE the amount of charge that is necessary to convert 50 % of the substrate – here the *n*-hexanoic acid - passed through the system. *n*-CA mixture solutions were prepared as described above for *n*-hexanoic acid solutions, using 10.48 g L^{-1} C_4, 37.42 g L^{-1} C_6 and 6 g L^{-1} C_8 resulting in an overall 0.48 M MCCA mixture with a molar ratio of (C_4 : C_6 : C_8: 1 : 2.67 : 0.34). Here, the *n*-CA mixture composition is based on the MCCA solution gained by Xu *et al.* from a two-stage microbial conversion of acid whey [14].

2.4. Quantification and analysis of liquid electrolysis products

After the Kolbe electrolysis the anolyte was kept closed at room temperature until further sample processing (between 1 - 3 days). A 50% H_2SO_4 solution was added to adjust the pH to ~ 2 to improve phase separation. For quantification of reaction products, the acidified anolyte was left for 2 h in a separating funnel. Thereafter, the organic phase was carefully separated, and diluted in *n*-hexane and in parallel in dichloromethane. Dilutions of 1:10, 1:100 and 1:1000 in both solvents were analysed. The dilution series of the organic phase were analysed via GC-MS (GC 7890A and MSD 5975C InertXL, Agilent, Santa Clara, USA). Quantification was carried out with external standards. Further details on the GC-MS method can be found in SI 2.4.

2.5. Data processing and calculations

2.5.1. Coulombic efficiencies

The Coulombic efficiency for each component i, CE_i, was derived from the charge Q_i in relation to the total charge (Q_{total}) introduced during electrolysis according to Eq. 1. Q_i was calculated from the consumed or produced amount of substance n_i within the anolyte (the volume was assumed to be constant):

$$CE_i = \frac{Q_i}{Q_{total}} \cdot 100\% \quad \text{Eq. 1}$$

with $Q_i = n_i \cdot z_i \cdot F$

where n_i is the amount of each substance in mol, z_i is the number of transferred electrons per molecule (see Tab. S2) and F = 96.485 C mol^{-1} is the Faraday constant. Q_{total} can be derived from the integrated current (i) that was set over time (Eq. 2):

$$Q_{total} = \int i(t)\, dt \quad \text{Eq. 2}$$

Additionally the CE_{fuel} of the electrolysis was calculated according to Eq. 3 from the sum of Q_i of all measured products in the organic phase (excluding unconverted C_6):

$$CE_{fuel} = \frac{\sum Q_{i,products}}{Q_{total}} \cdot 100\% \quad \text{Eq. 3}$$

2.5.2. Yield, selectivity and rates of the electrolysis

The *n*-decane yield, Y_{decane}, is given by Eq. 4. The gravimetrically determined molar amount of *n*-hexanoic acid before the electrolysis $n_{hexanoic\ acid,before}$ is used as the reference amount.

$$Y_{decane} = \frac{2 \cdot n_{decane}}{n_{hexanoic\ acid,before}} \cdot 100\% \quad \text{Eq. 4}$$

In order to assess the selectivity, S_{decane}, of the electrolysis of *n*-hexanoic acid to *n*-decane, the molar amount of *n*-decane was related to the amount of all measured products. Since the gas phase was not analysed the selectivity for *n*-decane considers only the products found in the liquid organic phase.

$$S_{decane} = \frac{n_{decane}}{\sum n_{products}} \cdot 100\% \quad \text{Eq. 5}$$

For determining the consumption rate (r_i) of *n*-hexanoic acid and the production rate of *n*-decane the consumed or produced mass of respective substance (Δm_i) was divided by the reaction volume ($V = 1\ \mathrm{L}$) and the electrolysis time (t) as well as the geometric electrode surface area ($A_{electrode\ surface}$).

$$r_i = \frac{\Delta m_i}{A_{electrode\ surface} \cdot V \cdot t} \quad \text{Eq. 6}$$

2.5.3. Statistical analysis

All experiments were performed with at least three independent replicates (n ≥ 3) for each condition. In this regard independent replicates means that the electrolysis of the n-hexanoic acid solution and the post electrolysis sample preparation and measurement were performed fully independently for each single replicate. All values are given as the mean ± Student t confidence interval (CI, α = 0.05).

3. Results and Discussion

3.1. Conversion of *n*-hexanoic acid in a technical scale single stack electrolysis cell

The results for the Kolbe electrolysis of *n*-hexanoic acid (C_6) in the single stack electrolysis cell are displayed in Fig. 3 and 4 as well as Fig. S4 and Tab. S3. Fig. S4 shows an overview of the range of reaction products (the resulting mixtures we call *fuel*) from C_6 electrolysis (orange and green bars). For all studied current densities (j) the Coulombic efficiency for fuel production (CE_{fuel}) is kept high (there is no statistical significant difference between the averages) when increasing the degree of conversion from 0.25 up to 0.5 FE. The CE_{fuel} then starts decreasing from degree of conversion of 0.5 to 1.5 FE (Fig. 3A and Tab. S3). This was expected, as the single stack electrolysis cell was operated in batch recirculation mode, which is equivalent to batch operation mode[31]. For low degrees of conversion, when the concentration of the substrate C_6 is high, the production rate of *n*-decane (r_{decane}), being the major Kolbe product from C_6 electrolysis, and CE_{fuel} remain high. For a higher degree of conversion, the C_6 concentration becomes limiting resulting in a lower r_{decane} and CE_{fuel}. This finding resembles first order and pseudo-first order reaction kinetics in batch reactors. As j increases from 150 to 450 mA cm^{-2} (at concomitantly increases in the cell voltage (E_{cell}), see Tab. S4) also the CE_{fuel} and the r_{decane} at 0.5 FE increase from an average CE_{fuel} = 44.5 ± 2.8 % at 150 mA cm^{-2} up to CE_{fuel} = 68.4 ± 29.6 % at 450 mA cm^{-2} (Fig. 3A and Tab. S3). Although being counter intuitive, this increase is related to the reaction mechanism of the charged C6 molecules at the anodic surface forming an increased hydrophobic layer that is expelling water and hence making the OER less likely, as further explained in [31].These efficiencies are well in line with or even higher than those of other studies performing the (non-)Kolbe electrolysis using electrochemical flow reactors. Kurig *et al.* reported a $CE_{product}$ of below 25 % for semi-batch conditions and 54 % for continuous mode

using monomethyl succinic acid as substrate[28]. Green *et al.* only achieved a $CE_{product}$ ≈ 10 % in a microfluidic electrolysis cell performing the Kolbe electrolysis of monomethyl succinate to dimethyl adipate[27]. Only Ziogas *et al.* achieved higher CE (likely based on substrate consumption) and selectivities (S) of more than 70 % and 90 % respectively[30]. However, they used a microfluidic electrochemical flow cell having only an active reactor volume of 0.138 cm^3 and an active electrode surface area of 6.912 cm^2 being not of technical relevance for production of bulk products like fuels. Comparing the results in the single stack electrolysis cell presented here with results from batch experiments from our previous publication CE_{fuel} of 58.9 ± 16.4 % for the Kolbe electrolysis of C_6 at the optimum degree of conversion of 0.5 FE was reported[32]. Additionally, a CE_{fuel} about 10 % higher can be achieved for a MCCA mixture with r_{fuel} = 0.009 ± 0.0006 mol cm^{-2} L^{-1} h^{-1} (equivalent to about 2.6 g L^{-1} h^{-1}) [31], being up to 28-fold lower than r_{decane} presented here (see Tab. S3). However, a more in-depth comparison with literature values is impossible, since reported values are usually only related to the conversion of the starting material ($CE_{substrate}$, $r_{substrate}$) and not to the amount of product or only the $Y_{product}$ is provided and the CE is disregarded.

Notably, the statistic variability of the CE_{fuel} also increases with increasing current density (Tab. S3). The 95 % confidence intervals for the higher j (i.e. 300, 450 mA cm^{-2}) remain high compared to the average values, and become much lower for j = 150 mA cm^{-2}. The CE_{fuel} at 150 mA cm^{-2} and 2 L min^{-1} recirculation for a conversion at 0.5 FE is higher (73.7 ± 3.1 %) than the CE_{fuel} at 150 mA cm^{-2} and 1 L min^{-1} (44.5 ± 2.8 %). This is a good indicator that mass-transfer regarding the gas evolution (that is decreasing the anodic active surface area) may be the cause for this disparity (see Fig. S3). At 2 L min^{-1} the expected trend of decrease of CE_{fuel} with the increase in current density is again visible, hinting this time for mass transport limitation of the substrate C6.

In line with the trends discussed for CE_{fuel} are the trends for r_{decane} that is the main product of the Kolbe electrolysis from C_6 (Fig. 3B and Tab. S3). As the degree of conversion increased from 0.25 up to 0.5 FE also r_{decane} increases, and decreases from 0.5 to 1.5 FE for all studied j. The highest r_{decane} for all j was achieved at 0.5 FE, with a maximum at 450 mA cm^{-2} yielding 0.732 ± 0.342 g L^{-1} h^{-1} cm^{-2} of *n*-decane. Similarly, as for the CE_{fuel} the r_{decane} suffers from increased statistical variability with increasing j (see Tab. S3).

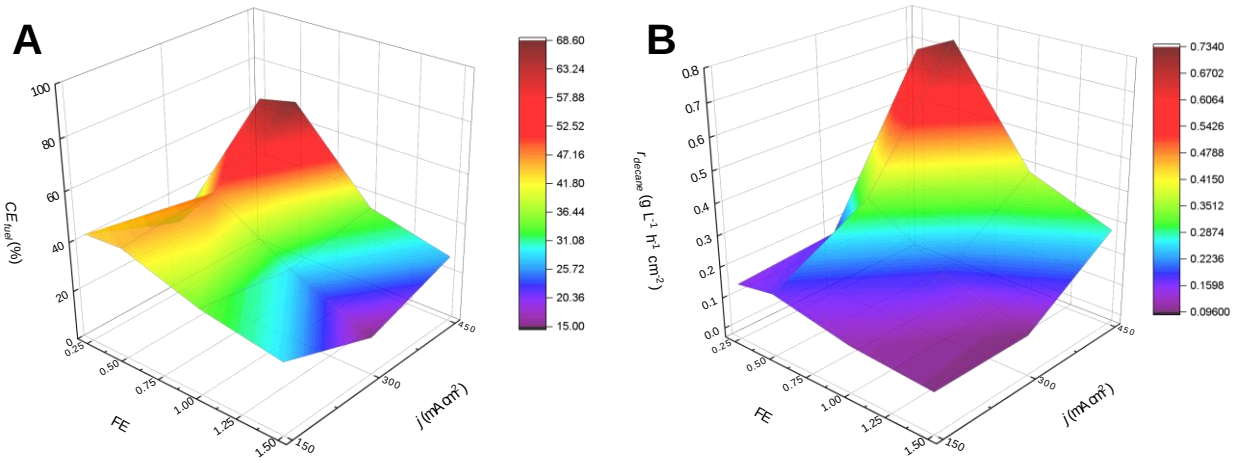
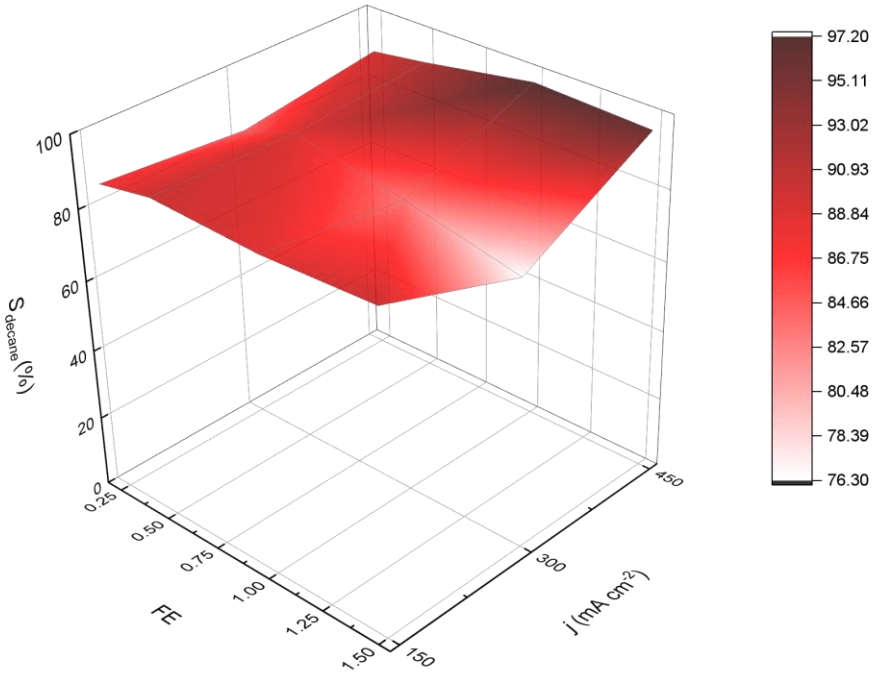


Figure 3: (A) Coulombic efficiency for fuel production, CE_{fuel} (%), and (B) *n*-decane production rate, r_{decane} (g L^{-1} h^{-1} cm^{-2}), from conversion of 0.52 M *n*-hexanoic acid (C_6) via Kolbe electrolysis while varying the degree of conversion from 0.25 to 1.5 FE and j from 150 to 450 mA cm^{-2} using the single stack electrolysis cell. Red areas resemble a high CE_{fuel}/r_{decane} while blue and purple resemble low CE_{fuel}/r_{decane}. The data used for plotting this graphic is shown in Tab. S3.

Fig. 4 shows the selectivity for *n*-decane, S_{decane}, relative to all liquid electrolysis products at different j and degrees of conversion. Overall, S_{decane} is between 76 % and 97 % regardless of the applied conditions and thus very high for all studied j. This is a good indicator for the high electrolysis reliability and noteworthy, the statistical variability for S_{decane} (Tab. S3) is not as high as for the CE_{fuel} and r_{decane} with increasing j.



278 **Figure 4:** Selectivity for *n*-decane, S_{decane} (%), obtained via the Kolbe electrolysis of 0.52 M *n*-hexanoic
279 acid (C_6) at different FE varied from 0.25 to 1.5 and different j varied from 150 to 450 mA cm^{-2} using the
280 single stack electrolysis cell. Dark red areas resemble a high S_{decane} while light red and white resemble low
281 S_{decane}. The data used for the graphic is shown in Tab. S3.
282
283 In order to bring this optimized system one step closer to using MCCA mixtures derived from biological
284 processes, the Kolbe electrolysis of an artificial mixture of *n*-carboxylic acids (*n*-CA) resembling one of the
285 best performing MCCA production by Xu *et al.* from a two-stage microbial conversion of acid whey, so far
286 [14]. Namely C_4, C_6 and C_8, at molar ratios of 1:2.67:0.34 respectively (0.48 M total acid concentration) was
287 performed in the 100 cm^2 single stack cell. For performing the Kolbe electrolysis of the mixture the same
288 optimized conditions previously found for 0.5 M C_6 solutions were applied: 150 mA cm^{-2}, 2 L min^{-1} anodic
289 recirculation rate and 0.5 FE of electric charge applied. The results are shown in Fig. S4. As it can be
290 expected, the product spectra of the liquid fuel shows a greater variety when using the artificial *n*-CA mixture
291 compared to the product spectra of the C_6 solutions [31]. This product variety is based on the formation of
292 different sized radical molecules and the possibility of a more diverse recombination of these, leading to
293 hetero-dimers derived from the different *n*-CA present, as well as homo-dimers. Eleven additional products

were detected for the *n*-CA mixture derived fuel: 5 esters, 2 alcohols and 4 alkanes. Among the detected products of electrolysis of the *n*-CA mixture only three exhibited a CE_i higher than 5%: *n*-decane with CE_i = 42 % (homo-dimer of C_6), *n*-dodecane with CE_i = 10 % (hetero-dimer of C_6 and C_8) and *n*-octane (hetero-dimer of C_4 and C_6) with CE_i = 6 %. The overall CE_{fuel} was slightly lower for the electrolysis of the mixture compared to the electrolysis of C_6 (67.5 % vs 73.7%, respectively). This might have been influenced by the observed foaming with the *n*-CA mixture, likely leading to slower mass transfer and thus lower substrate availability as well as decrease of active electrode surface area[33]. This may be overcome by optimizing electrode surface properties as well as improved reactor pumping/flow architecture [33, 34].

The liquid organic product from the electrolysis of 0.52 M C_6 solutions was analyzed for its fuel related properties and compared to gasoline and diesel as well as aviation fuel for turbine-engine jets (Tab. 1) [13]. It is important to underline that this analysis was performed with samples of the produced organic phase obtained and separated directly from the electrolysis mixture without the acidification step for enhancing the phase separation and without any down-stream processing (DSP) (incl. no drying etc.).

Table 1: Comparison between the properties of the fuel-like organic phase resulting from the Kolbe electrolysis of 0.52 M *n*-hexanoic acid (C_6) at 450 mA cm^{-2} and 0.5 FE in a single stack electrolysis cell and gasoline, diesel as well as kerosene.

Parameter	Gasoline[13]	Diesel[13]	Aviation fuel (turbine-engine)[35]	Kolbe fuel
Density (g mL^{-1})	0.720 - 0.775 (15°C)	0.820 - 0.845 (15°C)	0.751 - 0.845 (15°C/15.5°C) (≈ 0.745 - 0.805, 40°C)	0.8089 (40°C)
Kinematic viscosity at 40°C (mm^2 s^{-1})	0.5 - 0.6	2.0 - 4.5	0.74 - 1.3	1.43

Water content (g kg^{-1})	n.d.	0.2	n.d.	0.64
Higher heating value (MJ kg^{-1})	46.5 - 46.7	45.6	42.6 - 43.8	38.4
Sulfur content (g kg^{-1})	max. 0.01	max 0.01	max. 0.4 (w%)	<0.1
Oxygen content (% w/w)	max 2.7	n.d.	n.d.	n.d.
Carbon content (% w/w)	n.d.	86.2 - 86.6	n.d.	70.2
Hydrogen content (% w/w)	n.d.	13.1 - 13.5	13.5 - 14.4	13.0

n.d. refers to values that are not determined respectively not specified

Note: The samples of fuel for this analysis were not obtained by acidification of the electrolyzed samples. Instead, after electrolysis the organic phase was simply separated from the aqueous phase by decantation using a separation funnel.

The properties (i.e. density, viscosity, hydrogen content) of the obtained Kolbe fuel are more similar to diesel than gasoline. The actual composition (majorly *n*-decane) as well as the overall properties of the Kolbe fuel are most similar to aviation fuel for jet engines (kerosenes). Thus, most of the parameters show that the Kolbe fuel may be adequate for the utilization as drop-in biofuel in internal combustion engines, especially jet turbine engines. The higher heating value is lower than the values for gasoline and diesel (46.5 - 46.7 and 45.6 MJ kg^{-1} respectively vs. 38.4 MJ kg^{-1}) but relatively close to the value for aviation fuel (42.6 - 43.8 MJ kg^{-1} respectively). The difference of ~5 MJ kg^{-1} can be assigned to the higher water content in the here harvested Kolbe fuel compared to the petro-based fuels, as no pre-treatment beyond a careful phase separation with a decantation funnel and no DSP was done. This remaining water can easily be removed by established procedures at technical scale. Additionally, the Kolbe fuel, although majorly consisting of *n*-decane, also contains alcohols and esters in small relative amounts (see Tab. S2 and Fig. S4 in the SI) that may contribute to an overall lower higher heating value [36].

3.2. Power and energy considerations

In Tab. S4 and S5 energy calculations for the electrolysis of C_6 are shown using the here described single stack electrolysis cell at different conditions, i.e. j (150, 300 and 450 mA cm^{-2}) and recirculation flow rates

(1 and 2 L min^{-1}) for the optimum degree of conversion (0.5 FE). At this scale, 100 cm^2 anode surface area and 1 L anolyte volume, the Kolbe electrolysis achieves optimal energetic efficiencies, η, when conducted either at higher power and a low flow rate (450 mA cm^{-2}, 1 L min^{-1}) or at lower power and higher flow rate (150 mA cm^{-2}, 2 L min^{-1}) (see SI section 3.4.). Both cases require a similar specific energy consumption, E_{decane}, of 18.7 and 17.9 Wh g^{-1} for obtaining the major electrolysis product *n*-decane. This allows the selection between different batch times, here 0.4 h for 150 mA cm^{-2} or 0.13 h for 450 mA cm^{-2}, without the need to compromise on E_{decane}. Ziogas *et al.* reported a lower specific energy consumption for tailor-made jet fuel and diesel of 1.745 and 1.5 Wh g^{-1}, respectively using the Kolbe electrolysis of an artificial MCCA mixture[30]. However, the values can by far not be compared, as Ziogas *et al.* worked on the microscale (reactor volume of < 0.2 cm^3) and only took $P_{electrolysis}$ into account, being in their case 3- to 5-times lower compared to this study because of the use of a single-chamber system without membrane. We show that $P_{pumping}$ certainly needs to be considered at technical scale, as it does have a share of up to 50 % of P_{total} (see Tab. S4).

Thus, the energetic efficiency, η, of the Kolbe electrolysis of C_6 looks already very promising at the presented scale, also including $P_{pumping}$. Here, η around 27 % is estimated, considering *n*-decane as product and C_6 as substrate. If the input of energy contained in the substrate C_6 is disregarded, as it can be assumed for C_6 originating from a green bioprocess of waste water or biomass, the overall energetic efficiency is as high as 70%, being comparable to state of the art H_2 electrolyzers [37]. This opens up highly interesting possibilities for future process engineering and operation, for instance using Kolbe electrolysis only in case of the availability of “excess” grid electric energy. Furthermore, the here presented single stack electrolysis cell can be easily scaled and numbered-up to allow interfacing to technical scale biological MCCA production (see SI section 3.5.). For instance, when electrolyzing MCCA gained at technical scale as described by Xu *et al.* from acid whey being considered a waste stream in dairy industry [14], a fuel production of nearly 1 t per day can be estimated (SI 3.5.).

4. Conclusions

Using a single stack electrolysis cell for the Kolbe electrolysis of C_6 enabled the successful scale-up from a 2 cm^2 batch operation to 100 cm^2 recirculating batch operation resulting in a CE_{fuel} of nearly 70 % and r_{decane} ≈ 73 g L^{-1} h^{-1} at 450 mA cm^{-2} and 1 L min^{-1} flow rate (Tab. S3). This set of data is unprecedented in literature (see Tab. S7). Additionally, optimal combinations of j and flow rate were revealed allowing a variation of electrolysis time without losses in performance. Thereby, higher j result in increased fuel production rates at lower recirculation flow rates, especially for lower degrees of conversion. Compared to the previously performed batch experiments[32] the scale-up showed no performance losses. This will allow numbering-up at process relevant scale and conditions as well as interfacing to biological processes so that electrobiorefineries [13] come into reach. These electrobiorefineries can be integrated into existing production lines, but also allow decentralized operation.

It is important to mention that other green approaches using biomass, like triglycerides, lignocellulose, sugar or starch, for bio-based jet fuel production, e.g. hydroprocessed esters and fatty acids (HEFA), hydrotreated depolymerised cellulosic jet (HDCJ) or alcohol-to-jet, exist. Even if these processes look promising reaching Y and S up to 90 % they have other disadvantages like high temperature and pressure during catalysis, the need to continuously feed H_2 as additional substrate, resilient feedstocks or feedstocks that are edible crops [38]. Additionally, η of these approaches does not exceed 1 % yet [39]. Other approaches don't use biomass as substrate for the production of green fuel but instead CO_2 and H_2 which can be captured from the air and be produced via water electrolysis respectively. Therefore, catalysts like Fe-Mn-K or Y-type zeolites with cobalt nanoparticles are used to reach CO_2 conversion efficiencies of 38.2 %, $Y_{C_{5+}}$ of 22.3 % and $S_{product}$ between 45 - 74 % [40]. Also thermochemical fuel production using sunlight and H_2O and CO_2 from air is possible but also only reaches η below 1 % [41]. Thus, as it can be seen from the examples presented, the electrochemical production of drop-in fuel as well as fuel additive for aviation from MCCA is with S_{decane} between 76 % and 97 % well in line with the $S_{product}$ of alternative approaches. It already shows a high η above 25 % and still offers possibilities for improvement e.g. continuous operation mode or the use of other MCCA mixtures, and is therefore one of the most promising approaches for decarbonisation of the mobility sector.

Acknowledgements

This research is financed by the German Federal Ministry of Education and Research (BMBF) under the VIP+-project MolkeKraft: Microbial-electrochemical exploitation of sour whey for the production of drop-in aviation fuel [Funding code: 03VP06911].The responsibility for the content lies with the authors. This work was supported by the Helmholtz-Association in the frame of the Integration Platform “Tapping nature’s potential for sustainable production and a healthy environment” at the UFZ. We thank Dr. Micjel Chávez Morejón and Mrs. Angelika Wichman from our department for their diligence and assistance with the analytics, and to Dr. Jana Mühlenberg from the Deutsches Biomasseforschungszentrum gemeinnützige GmbH Leipzig for her measurements of the fuel properties.

Declaration of interests

The authors declare no competing interests.

References

[1] https://ourworldindata.org/emissions-by-sector.

[2] https://www.ev-volumes.com/country/total-world-plug-in-vehicle-volumes/.

[3] https://europe.autonews.com/automakers/germany-backs-eu-phaseout-new-combustion-engine-cars.

[4] L.M. Thomas Earl, Stef Cornelis, Samuel Kenny, Carlos Calvo Ambel, James Nix, Analysis of long haul battery electric trucks in EU Marketplace and technology, economic, environmental, and policy perspectives., Amended paper (August 2018) originally presented in: 8th Commercial Vehicle Workshop (2018).

[5] D. Castelvecchi, Electric Cars: The Battery Challenge, Nature 596(7872) (2021) 336-339. https://doi.org/10.1038/d41586-021-02222-1.

[6] https://www.mckinsey.com/industries/automotive-and-assembly/our-insights/how-hydrogen-combustion-engines-can-contribute-to-zero-emissions.

[7] K.Y. Show, Y.G. Yan, C.X. Zong, N. Guo, J.S. Chang, D.J. Lee, State of the art and challenges of biohydrogen from microalgae, Bioresource Technol 289 (2019). https://doi.org/10.1016/j.biortech.2019.121747.

[8] https://afdc.energy.gov/fuels/properties.

[9] A. Bauen, N. Bitossi, L. German, A. Harris, K. Leow, Sustainable Aviation Fuels Status, challenges and prospects of drop-in liquid fuels, hydrogen and electrification in aviation, Johnson Matthey Tech 64(3) (2020) 263-278. https://doi.org/10.1595/205651320x15816756012040.

[10] Ways to make aviation fuel green, Science & Technology Supplement: Air travel. The Economist (2022).

[11] https://www.caafi.org/focus_areas/fuel_qualification.html.

[12] E.K. Stefan Zoller, Dustin Nizamian, Marco Stephan, Adriano Patané, Philipp Haueter, Manuel Romero, José González-Aguilar, Dick Lieftink, Ellart de Wit, Stefan Brendelberger, Andreas Sizmann, AldoSteinfeld, A solar tower fuel plant for the thermochemical production of kerosene from H2O and CO2, Joule 6(7) (2022) 10.

[13] C. Urban, J.J. Xu, H. Strauber, T.R.D. Dantas, J. Muhlenberg, C. Hartig, L.T. Angenent, F. Harnisch, Production of drop-in fuels from biomass at high selectivity by combined microbial and electrochemical conversion, Energ Environ Sci 10(10) (2017) 2231-2244. https://doi.org/10.1039/c7ee01303e.

[14] J.J. Xu, J.X. Hao, J.J.L. Guzman, C.M. Spirito, L.A. Harroff, L.T. Angenent, Temperature-Phased Conversion of Acid Whey Waste Into Medium-Chain Carboxylic Acids via Lactic Acid: No External e-Donor, Joule 2(2) (2018) 280-295. https://doi.org/10.1016/j.joule.2017.11.008.

[15] A. Duber, L. Jaroszynski, R. Zagrodnik, J. Chwialkowska, W. Juzwa, S. Ciesielski, P. Oleskowicz-Popiel, Exploiting the real wastewater potential for resource recovery - n-caproate production from acid whey, Green Chem 20(16) (2018) 3790-3803. https://doi.org/10.1039/c8gc01759j.

[16] T.A. Gehring, W.A. Cavalcante, A.S.C. Eng, L.T. Angenent, S.T. Santaella, M. Lubken, R.C. Leitao, Optimal pH set point for simultaneous production and pertraction of n-caproic acid: an experimental and simulation study, J Chem Technol Biot 95(12) (2020) 3105-3116. https://doi.org/10.1002/jctb.6486.

[17] C.A. Contreras-Davila, V.J. Carrion, V.R. Vonk, C.N.J. Buisman, D.P.B.T.B. Strik, Consecutive lactate formation and chain elongation to reduce exogenous chemicals input in repeated-batch food waste fermentation, Water Res 169 (2020). https://doi.org/ARTN 115215
10.1016/j.watres.2019.115215.

[18] L.A. Kucek, M. Nguyen, L.T. Angenent, Conversion of L-lactate into n-caproate by a continuously fed reactor microbiome, Water Res 93 (2016) 163-171. https://doi.org/10.1016/j.watres.2016.02.018.

[19] J. Chwialkowska, L. Smaga, P. Oleskowicz-Popiel, Operating parameters in open culture fermentation of sugars, Biosyst Eng 210 (2021) 78-90. https://doi.org/10.1016/j.biosystemseng.2021.08.002.

[20] T.I.M. Grootscholten, K.J.J. Steinbusch, H.V.M. Hamelers, C.J.N. Buisman, Improving medium chain fatty acid productivity using chain elongation by reducing the hydraulic retention time in an upflow anaerobic filter, Bioresource Technol 136 (2013) 735-738. https://doi.org/10.1016/j.biortech.2013.02.114.

[21] Q.L. Wu, X. Bao, W.Q. Guo, B. Wang, Y.X. Li, H.C. Luo, H.Z. Wang, N.Q. Ren, Medium chain carboxylic acids production from waste biomass: Current advances and perspectives, Biotechnol Adv 37(5) (2019) 599-615. https://doi.org/10.1016/j.biotechadv.2019.03.003.

[22] L.A. Kucek, C.M. Spirito, L.T. Angenent, High n-caprylate productivities and specificities from dilute ethanol and acetate: chain elongation with microbiomes to upgrade products from syngas fermentation, Energ Environ Sci 9(11) (2016) 3482-3494. https://doi.org/10.1039/c6ee01487a.

[23] T.I.M. Grootscholten, K.J.J. Steinbusch, H.V.M. Hamelers, C.J.N. Buisman, Chain elongation of acetate and ethanol in an upflow anaerobic filter for high rate MCFA production, Bioresource Technol 135 (2013) 440-445. https://doi.org/10.1016/j.biortech.2012.10.165.

[24] J.M. Carvajal-Arroyo, S.J. Andersen, R. Ganigue, R.A. Rozendal, L.T. Angenent, K. Rabaey, Production and extraction of medium chain carboxylic acids at a semi-pilot scale, Chem Eng J 416 (2021). https://doi.org/10.1016/j.cej.2020.127886.

[25] J.E. Sanderson, P.F. Levy, L.K. Cheng, G.W. Barnard, The Effect of Pressure on the Product Distribution in Kolbe Electrolysis, J Electrochem Soc 130(9) (1983) 1844-1848. https://doi.org/Doi 10.1149/1.2120109.

[26] P.F. Levy, J.E. Sanderson, L.K. Cheng, Kolbe Electrolysis of Mixtures of Aliphatic Organic-Acids, J Electrochem Soc 131(4) (1984) 773-777. https://doi.org/Doi 10.1149/1.2115697.

[27] R.A. Green, R.C.D. Brown, D. Pletcher, Electrosynthesis in Extended Channel Length Microfluidic Electrolysis Cells, J Flow Chem 6(3) (2016) 191-197. https://doi.org/10.1556/1846.2016.00028.

[28] N. Kurig, J. Meyers, E. Richter, S. Palkovits, R. Palkovits, 3D Printed Microreactors for the Continuous Non-Kolbe Electrolysis, Chem-Ing-Tech 94(5) (2022) 786-790. https://doi.org/10.1002/cite.202100178.

[29] N. Kurig, J. Meyers, F.J. Holzhauser, S. Palkovits, R. Palkovits, (Non-)Kolbe Chemistry Going with the Flow: The Continuous Electrolysis of Biogenic Acids, Acs Sustain Chem Eng 9(3) (2021) 1229-1234. https://doi.org/10.1021/acssuschemeng.0c06982.

[30] A. Ziogas, H. Pennemann, G. Kolb, Electrochemical Synthesis of Tailor-Made Hydrocarbons from Organic Solvent Free Aqueous Fatty Acid Mixtures in a Micro Flow Reactor, Electrocatalysis-Us 11(4) (2020) 432-442. https://doi.org/10.1007/s12678-020-00600-3.

[31] K. Neubert, M. Hell, M.C. Morejon, F. Harnisch, Hetero-Coupling of Bio-Based Medium-Chain Carboxylic Acids by Kolbe Electrolysis Enables High Fuel Yield and Efficiency, Chemsuschem (2022). https://doi.org/10.1002/cssc.202201426.

[32] K. Neubert, M. Schmidt, F. Harnisch, Platinized Titanium as Alternative Cost-Effective Anode for Efficient Kolbe Electrolysis in Aqueous Electrolyte Solutions, Chemsuschem 14(15) (2021) 3097-3109. https://doi.org/10.1002/cssc.202100854.

[33] A. Angulo, P. van der Linde, H. Gardeniers, M. Modestino, D.F. Rivas, Influence of Bubbles on the Energy Conversion Efficiency of Electrochemical Reactors, Joule 4(3) (2020) 555-579. https://doi.org/10.1016/j.joule.2020.01.005.

[34] D. Klüh, W. Waldmüller, M. Gaderer, Kolbe Electrolysis for the Conversion of Carboxylic Acids to Valuable Products—A Process Design Study., Clean Technologies 3(1) (2021) 1-18.

[35] P. Coordinating Research Council Inc., USA, Aviation fuel properties, Report n. 530 (1983).

[36] D.H. Qi, W.Q. Xing, P. Luo, J.H. Liu, R. Chen, Effect of alcohols on combustion characteristics and particle size distribution of a diesel engine fueled with diesel-castor oil blended fuel, Asia-Pac J Chem Eng 15(4) (2020). https://doi.org/10.1002/apj.2477.

[37] IRENA (2020), Green Hydrogen Cost Reduction: Scaling up Electrolysers to Meet the 1.5ºC Climate Goal, International Renewable Energy Agency, Abu Dhabi, ISBN: 978-92-9260-295-6.

[38] F.I.G.-C. C.Gutiérrez-Antonio, J.A.de Lira-Flores, S.Hernández, A review on the production processes of renewable jet fuel, Renewable and Sustainable Energy Reviews 79 (2017) 20.

[39] H.J. Wei, W.Z. Liu, X.Y. Chen, Q. Yang, J.S. Li, H.P. Chen, Renewable bio-jet fuel production for aviation: A review, Fuel 254 (2019). https://doi.org/10.1016/j.fuel.2019.06.007.

494 [40] B.Z. Yao, T.C. Xiao, O.A. Makgae, X.Y. Jie, S. Gonzalez-Cortes, S.L. Guan, A.I. Kirkland, J.R. Dilworth,
495 H.A. Al-Megren, S.M. Alshihri, P.J. Dobson, G.P. Owen, J.M. Thomas, P.P. Edwards, Transforming carbon
496 dioxide into jet fuel using an organic combustion-synthesized Fe-Mn-K catalyst, Nat Commun 11(1) (2020).
497 https://doi.org/10.1038/s41467-020-20214-z.

498 [41] R. Schappi, D. Rutz, F. Dahler, A. Muroyama, P. Haueter, J. Lilliestam, A. Patt, P. Furler, A. Steinfeld,
499 Drop-in fuels from sunlight and air, Nature (2021) 63-+. https://doi.org/10.1038/s41586-021-04174-y.